Available online at www.sciencedirect.com

ScienceDirect

Procedia Engineering00 (2014) 000–000

Procedia Engineering

www.elsevier.com/locate/procedia

23rd International Meshing Roundtable (IMR23)

Quality index and improvement of the interfaces of general hybrid grids

S. Fotia[a], Y. Kallinderis[a,*]

[a] *Laboratory for Aerodynamic Design of Air Vehicles,Department of Mechanical and Aeronautical Engineering,University of Patras, 26504 Rio, Greece*

Abstract

Hybrid grids constitute a significant class of meshes for complex-geometry flow simulations. They consist of prisms and/or hexahedra covering viscous regions primarily, while tetrahedra discretize the rest of the domain with pyramids serving as transitional elements. The local changes in element topology form grid interfaces. This is especially so for cases where the number of prisms/hexahedra per layer (stack) is not constant ("chopped" layers). The present work deals with the quality of the interfaces encountered in general hybrid grids with non-constant number of layers. *A priori* estimation of the quality is based on truncation error terms. Four representative types of interfaces are considered. The effect of grid stretching and skewness was examined for the interfaces. Further, the quality is improved via repositioning of the central point of each of the interface types. The improvement is quantified via application to several hybrid grids.

Keywords: Hybrid grid interfaces, Mesh quality, Truncation error, Mesh improvement

1. Introduction

The need for field simulations that involve complex physics and geometries poses a formidable challenge to grid generation [1,2]. Hybrid grids are a broad category of meshes, and are advantageous when demanding automatic grid generation for complex configurations [3-5]. Prismatic and hexahedral elements are created for the regions of boundary layers, while tetrahedra are used over the rest of the domain. Pyramids are employed as connecting

* Corresponding author.
E-mail address: kallind@otenet.gr

elements between the prismatic and hexahedral elements and the tetrahedra. Those areas constitute the interface regions where different types of elements create the local control volumes for the Finite Volume space discretization. There is little previous research on mesh quality measures and improvement for the interfaces [6-11]. The present work is intended to contribute in this area.

A key component of a grid generator is its mesh quality metrics. Those are necessary as: (i) requirement specifications during the mesh generation, (ii) guides of mesh improvement techniques, and (iii) sensors in grid adaptation procedures. Two broad categories of mesh quality indicators are: (i) *a priori* and (ii) *a posteriori* estimation. The first does not make use of solution field information and looks into the grid element metrics. The second "works" with the solution. *A posteriori* metrics are usually solution error indicators [12-17]. *A priori* grid quality assessment has been based primarily on geometric characteristics of the elements such as ratios of sizes of neighboring elements, as well as on element shape measures, such as angles of the elements [18-20]. In the Finite Element method, the quality of a mesh is often given in terms of the element/mesh regularity [21].

The present work has a dual purpose. First, it introduces *a priori* mesh quality index for interfaces of a general hybrid mesh derived from the analytic expression of the truncation error. Second, the study focuses on the interface region of the general hybrid grids. The relative research on quality measures and improvement devoted to hybrid grids is limited, especially for the interface region.

The truncation error (TE) is an important indicator of mesh quality. Direct relations between TE and mesh distortion parameters, such as departure from orthogonality, skewness and uniformity have been reported in [22]. However, despite the large number of studies on the relation of TE to the numerical solution [23,24], there have been few derivations of mesh quality measures based on it [7,8].

The present effort is based on previous work for two-dimensional hybrid grids [8]. This work was evaluated in [25], and presented favorable agreement between numerical error and the mesh quality indicators derived in [8]. This was a motivation for the extension to three-dimensions [7], and further to focus the work on the quality assessment of interfaces of three-dimensional hybrid grids, as well as on its improvement.

The following section 2 presents the mesh quality index. Next, section 3 lists the common types of the interfaces for general hybrid grids, followed by an assessment of their quality. Section 4 presents a quality improvement technique for the interfaces. Finally, section 5 contains the summary and the future work.

2. Mesh quality index for hybrid grids using truncation error terms

The goal of the present work is the quality assessment of the interfaces of general hybrid grids, using quality measures derived from the analytic expression of the truncation error (TE).

2.1. Analytic expression of the truncation error

A cell-vertex Finite Volume discretization of first order spatial derivatives will be the vehicle for defining the quality of general hybrid mesh in three dimensions. The discretization of first order derivatives is a common calculation for many field equations in Physics. A low order discretization was chosen on purpose so as to "bring out" the bad elements more clearly.

The truncation error (TE) in the calculation of the first order derivative is defined as the difference between the numerical and the analytical values of the gradients. Using Taylor series expansion for the field variable u, the truncation error is cast in the following general form:

$$\begin{aligned}\mathrm{TE} &= \left(e_x u_x + e_y u_y + e_z u_z\right) + \\ &\left(e_{xx} u_{xx} + e_{yy} u_{yy} + e_{zz} u_{zz} + e_{xy} u_{xy} + e_{zx} u_{zx} + e_{zy} u_{zy}\right) + \ldots\end{aligned} \tag{1}$$

The error terms (e) contain grid metrics only. These terms will be the basis for the *a priori* evaluation of mesh quality. The general form of the error coefficients of the Finite Volume discretization method is:

$$e_{x^{m_x} y^{m_y} z^{m_z}} = \frac{1}{V}\frac{k}{(m_x+m_y+m_z)!}\sum_f\left[\frac{\left(\Delta X_1^{m_x}\Delta Y_1^{m_y}\Delta Z_1^{m_z}+\ldots+\Delta X_N^{m_x}\Delta Y_N^{m_y}\Delta Z_N^{m_z}\right)}{N}S\right]_f \tag{2}$$

where $\sum_f$ is the summation over the external faces of the local control volume surrounding the grid point of interest, N is number of vertices which participate in the calculation of the average value of u for each face, S is the area of each face, and V the volume of the local control volume. Also, m_x, m_y, and m_z are integers equal to the order of the derivative of u with respect to *x*, *y*, and *z*, respectively. Finally, *k* is an integer coefficient from the Taylor expansion.

The equation (2) relates the truncation error to the mesh points coordinates. This will be the vehicle for making a direct connection between TE and mesh quality of a hybrid grid.

2.2. Mesh quality index for hybrid grids

The contribution of the local mesh topology to the truncation error is the focus of the present work. A quality index for general hybrid 3-D meshes will be used with the following properties: (i) it is a local index, one value of index for each one node of the mesh, (ii) direct derivation from the truncation error, (iii) relatively simple to compute for realistic cases, (iv) independent from the local mesh size so that the contribution of the mesh shape and topology is brought out.

The general form of the error coefficients (*EC*) of equation (2) can be employed to yield the value of the mesh quality index (Q). This is carried out using the absolute values of the first order *EC* terms:

$$\mathrm{Q}_i = \frac{\left|e_{xx}\right|+\left|e_{yy}\right|+\left|e_{zz}\right|+\left|e_{xy}\right|+\left|e_{zx}\right|+\left|e_{zy}\right|}{L_i} \tag{3}$$

where L_i is a local characteristic length for the normalization that has been introduced in [8], and *i* denotes the calculation of the *x, y*, or *z*-spatial derivative of the field function. Thus, the mesh quality index is defined as:

$$\mathrm{Q} = \mathrm{Q}_x + \mathrm{Q}_y + \mathrm{Q}_z \tag{4}$$

A zero value of Q is the ideal value of the above index.

An application of the suggested index in a hybrid mesh around a 3-D cylinder is shown in Fig. 1. The boundary layer region contains relatively uniform hexahedra so the quality index takes its optimum value (close to zero). Deterioration of quality is observed in the interface region and in the farfield, where the values of Q are quite larger than zero.

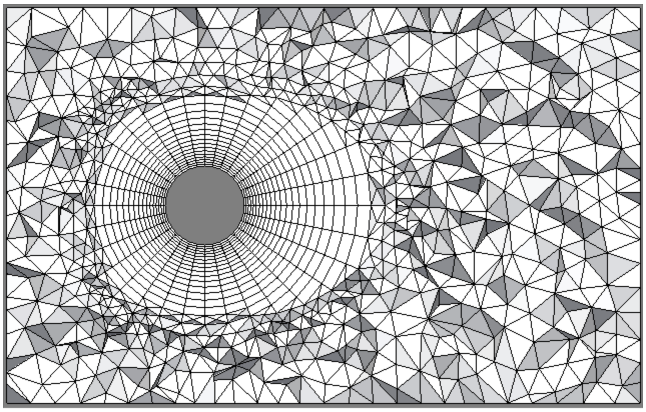

(a)

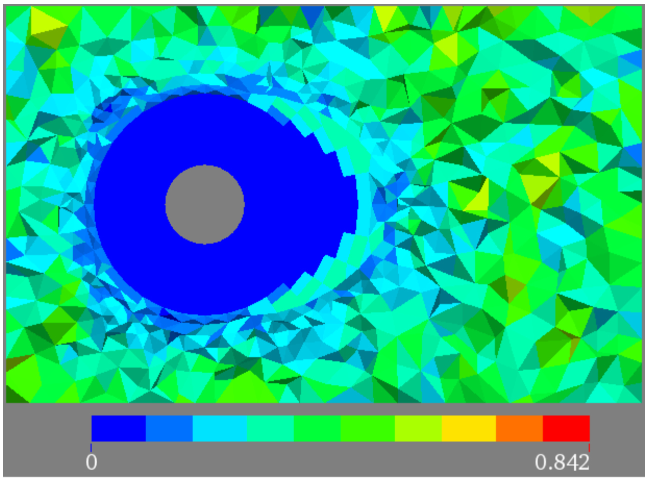

(b)

Fig. 1. Case of a 3-D cylinder: (a) Hybrid grid fieldcut, and (b) the corresponding distribution of the mesh quality index (Q).

3. Elementary types of hybrid grid interfaces for variable number of hexahedra stacks

The previous work [7] focused on the quality of “regular” hybrid grid interfaces, that are encountered in hybrid grids with constant number of layers of prisms/hexahedra. The present work is focused on realistic interfaces that contain variable number of prisms/hexahedra stacks (“chopping”). There are three primary “chopping” types: (i) node-based, (ii) multiple node-based, and (iii) edge-based chopping.

Node-based chopping of the layers frequently originates at a single point and then spreads out in all directions. This contains the interface cases of Fig. 2(a), 2(c), and 2(d). For example, those can be encountered in the junction between the trailing edge of a wing and the fuselage.

Multiple node-based chopping can occur when layer chopping originates at two or more points and then spreads out between the points. The interfaces of Fig. 2(b) can fall in this category. Such interfaces can be encountered, for example, in the aircraft tail region where there is chopping due to both the trailing edge of the vertical tail plane, and the horizontal tail plane.

Finally, in edge-based chopping the layer reduction originates along a sequence of edges and spreads out away from this line. The case of Fig. 2(b) is typical for edge-based chopping.

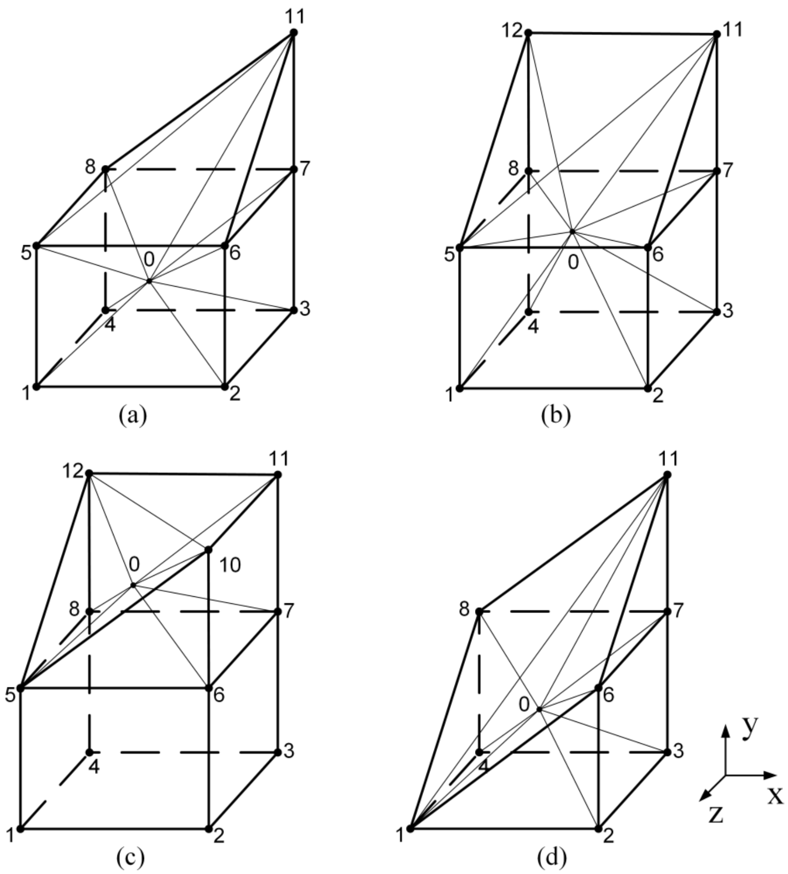

Fig. 2. Hybrid grid interfaces corresponding to hexahedra boundary layer grid with non-constant number of layers ("chopped" hexahedra). Cases of: (a) one base pyramid, four side pyramids, two side tetrahedra, and two top tetrahedra, (b) one base pyramid, five side pyramids, two side tetrahedra, and two top tetrahedra, (c) one base pyramid, two side pyramids, two side tetrahedra, and two top tetrahedra, and (d) one base pyramid, two side pyramids, four side tetrahedra, and two top tetrahedra.

The value of the mesh quality indices for the interfaces depicted in Fig. 2, is listed in Table 1. The quality index in each direction is included. It is observed that the indices in the *x*- and *z*-directions are equal due to the orientation of the interface elements. The quality in the "normal" (*y*) direction is worse than the "lateral" one.

Table 1. Mesh quality index values for the hybrid grid interfaces.

Interface Type	$Q_x = Q_z$	Q_y	Q
Fig. 2(a)	0.15	0.42	0.72
Fig. 2(b)	0.33	0.50	1.16
Fig. 2(c)	0.60	0.60	1.80
Fig. 2(d)	0.54	0.86	1.95

Next, the effect of stretching and skewness on the four types of interfaces is studied. Figure 3 defines the two distortions. Stretching is quantified as the ratio h_1/h_2, while skewness is measured via the angle ω.

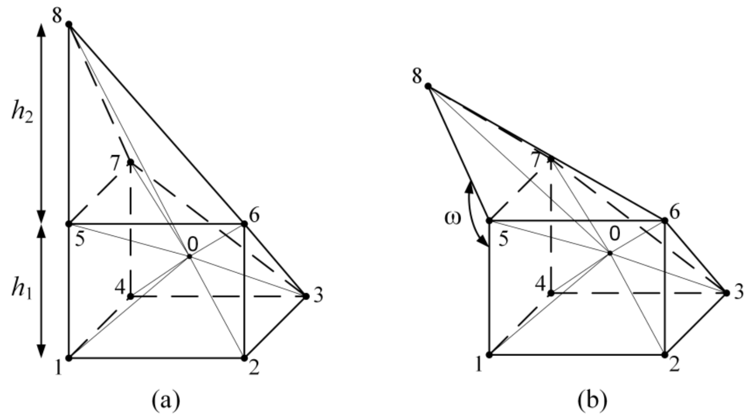

Fig. 3. Distortions of the interfaces: (a) unequal layer heights ($h_1 \neq h_2$), and (b) skewness ($\omega \neq 180^0$) between the layers.

Some degree of stretching (h_2/h_1) “helps” the quality of the interface types 2(b) and 2(d) as shown in Fig. 4. This improvement is due to the volumes of the elements below and above the interface surface becoming more equal. The other two types (2(a) and 2(c)) “see” a deterioration of their quality from the beginning.

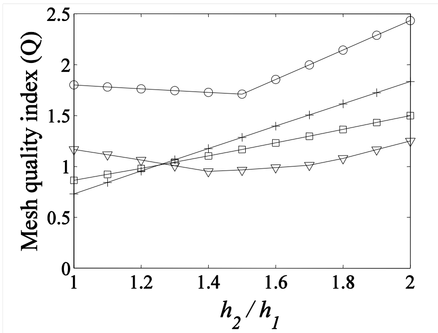

Fig. 4. Mesh quality index (Q) vs. the variation of layer heights (h_2/h_1) for the interfaces of Fig. 2: case of Fig. 2 (a) (+), case of Fig. 2(b) (∇) , case of Fig. 2(c) (□), and case of Fig. 2(d) (○).

Different degree of sensitivity to skewness is observed in Fig. 5. The interface types of Fig. 2(a) and 2(d) have relatively constant Q-values with increasing ω, while types 2(b) and 2(c) exhibit strong sensitivity of their quality to skewness.

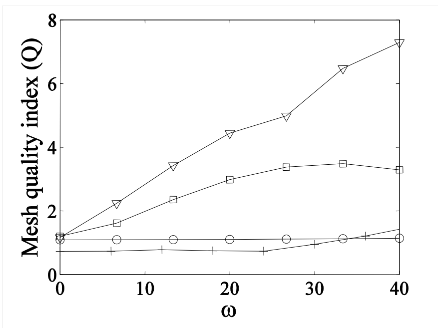

Fig. 5. Mesh quality index (Q) vs. skewness angle (ω) for the interfaces of Fig. 2: case of Fig. 2 (a) (+), case of Fig. 2(b) (∇) , case of Fig. 2(c) (□), and case of Fig. 2(d) (○).

4. Improvement of the interfaces via appropriate central point displacement

The present section deals with improvement of the quality of the hybrid mesh interfaces via movement of interface points. Following experimentation with various motions, it was found that repositioning of the central interface point 0 results in improved quality. Two are the criteria to assess the effectiveness of the point displacement: (i) the values of the quality index (Q), and (ii) an error that is calculated based on evaluation of the solution gradient using the Finite Volume discretization (*computed error*).

The central interface point is moved along the straight line between its initial position and the centroid of its node-dual volume. This polyhedral volume is the union of the grid elements sharing the central point. Figure 6 illustrates the initial and the final locations of point 0 for one of the types of the interfaces studied. The corresponding variation in the quality index (Q) is shown in Fig. 7 for all four types of interfaces. The parameter s_0 denotes the degree of the displacement as a fraction of the interface characteristic length (h) which is illustrated in Fig. 6(a).

In three of the four types of interfaces, the value of Q decreases until the central point has moved around the location of the centroid (Fig. 7). For the fourth type, that of Fig. 2(d), the values remain approximately constant up to $s_o \approx 0.15$. The degree of the reduction in Q (increase in quality) varies with that of interface type of Fig. 2(c) being the largest.

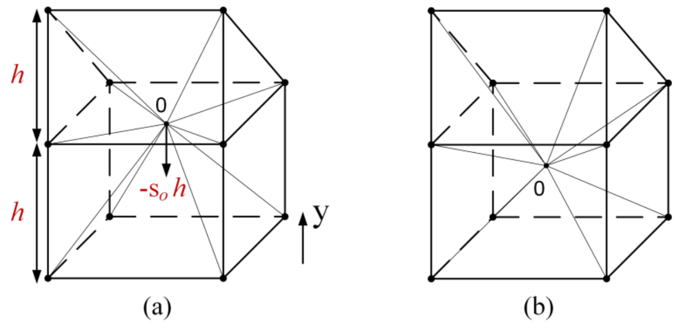

Fig. 6. Hybrid grid interface quality improvement: (a) initial configuration, and (b) the resulting mesh after movement of the central point (0).

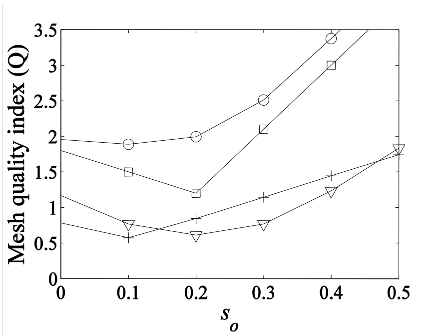

Fig. 7. Interface mesh improvement by applying central point movement. Mesh quality index (Q) vs. the central point movement (s_0). Cases of the four interface types: Fig. 2 (a) (+), Fig. 2(b) (∇) , Fig. 2(c) (□), and Fig. 2(d) (○).

Next, the central interface point repositioning is applied to a spectrum of hybrid grids created via the CENTAUR grid generator [26]. The grids are shown in Fig. 8 and include the following: (a) hybrid mesh over a bump with local stretching applied to leading edge area, (b) very thin boundary layer mesh over the bump, (c) grid around a rectangular barrier covering the entire span of the domain (z-direction), (d) hybrid mesh around a 3-D obstacle in the shape of a plate, and (e) hybrid mesh around an aircraft type of configuration. The case (d) of the plate includes two extra variants, namely the obstacle being extended at fullspan, and also the plate mesh being globally refined. The grids contain local irregularities by design so as to “trigger” relatively large values of Q.

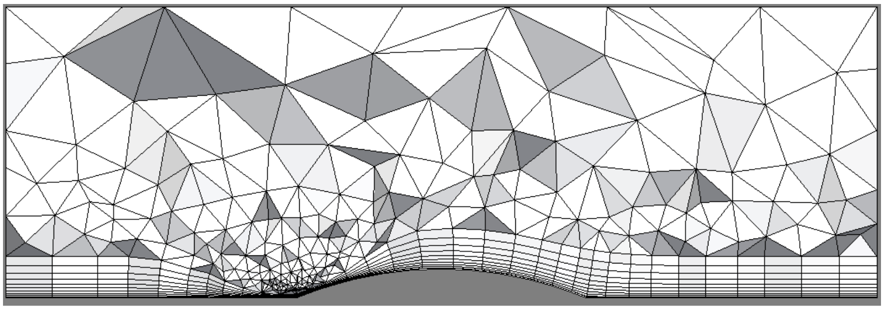

(a)

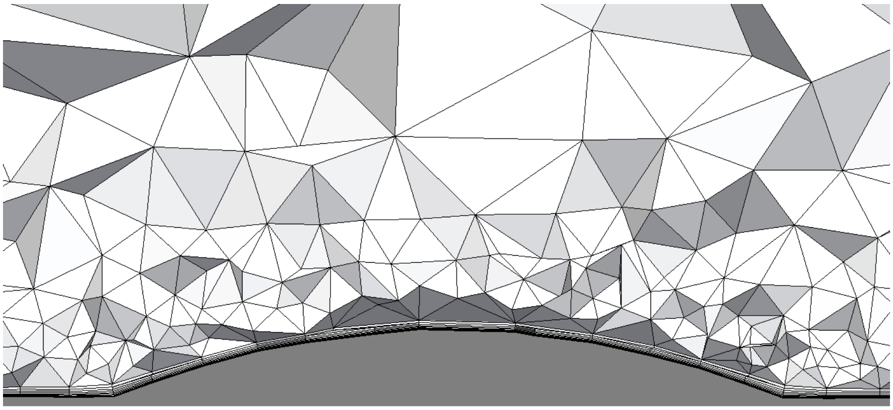

(b)

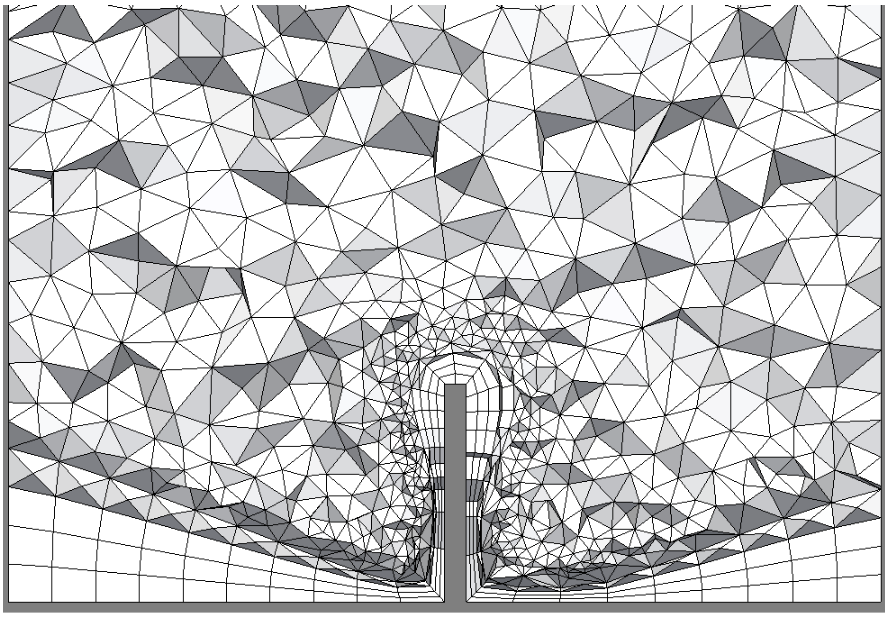

(c)

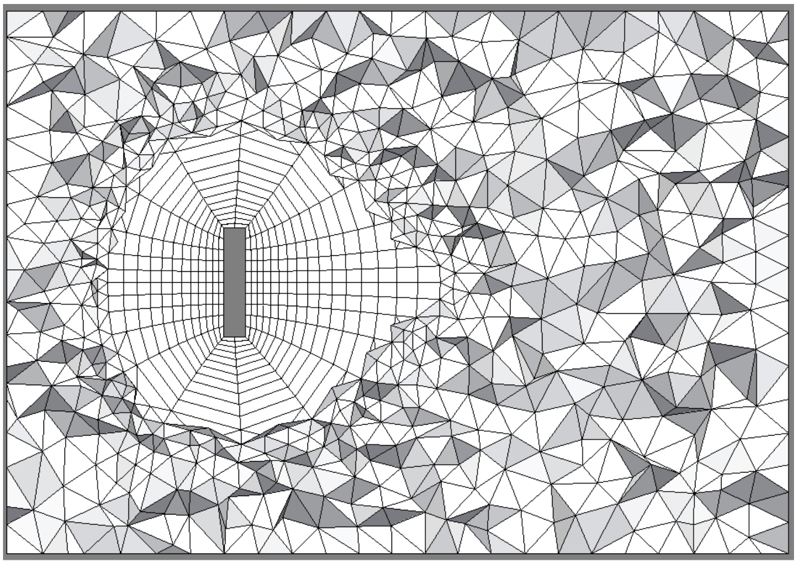

(d)

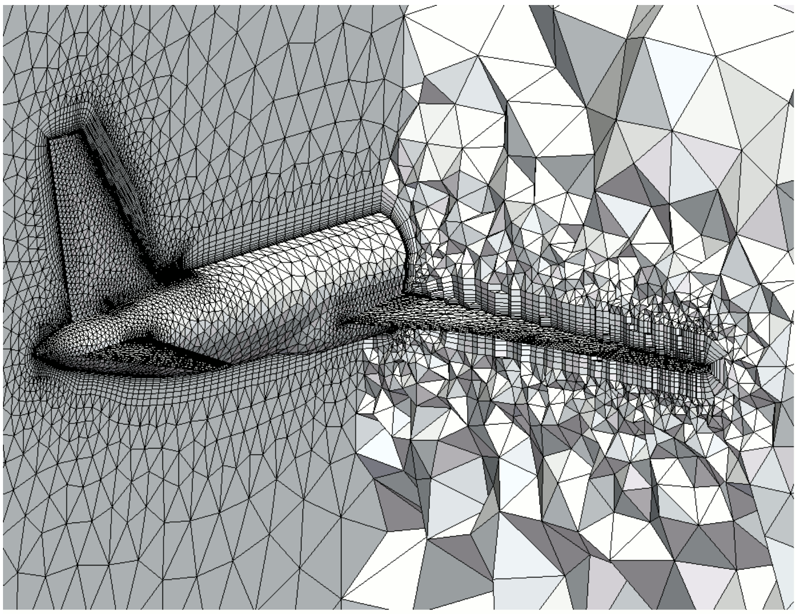

(e)

Fig. 8. Hybrid grids around: (a) a bump with local stretching at its leading edge, (b) bump with a thin prismatic mesh, (c) a barrier, (d) a plate, and (e) an aircraft.

The central point in all the interfaces of each of the grids presented is now repositioned until the corresponding value of its quality index (Q) is minimized. The values of Q at all the interface points are also monitored. An "interface point" is a point that belongs to different element types (prisms, hexahedra, tetrahedral and pyramids).

Table 2 lists all cases with the corresponding quality improvement. Two measures of quality are presented: (i) the average values of Q over all the interface points, and (ii) the maximum value of Q among all the interface points. It is observed that the quality is improved for the majority of the points (see first column). The second column shows the average Q improvement as a percentage. Appreciable reduction in Q on the average is observed for most cases.

The maximum value of Q over all the interface points is reduced for all cases as depicted in the last column of the table.

Table 2. Effect on the mesh quality (Q) of the movement of the central interface node.

Grid interfaces	Percentage of the interface nodes with their quality improved (%)	Improvement of the average quality (Q) of the interface nodes (%)	Reduction of the maximum Q at interface region after applying central point movement (%)
Bump Fig.8(a)	98.85	23.53	14.28
Bump Fig.8(b)	100.00	17.23	22.22
Barrier	70.67	14.81	31.57
Plate	74.82	27.58	36.36
Plate (refined)	79.73	26.82	24.00
Plate (fullspan)	74.69	12.90	17.74
Aircraft	68.04	3.65	42.85

Another metric of quality improvement that is employed is the computation of the solution gradient ($\vec{\nabla}\cdot\vec{u}$) via the Finite Volume method. An analytic field function ($\vec{u}$) is employed which results in defining a local error that can be used to further evaluate the effectiveness of the central point repositioning.

Specifically, for an incompressible flow field it is $\vec{\nabla}\cdot\vec{u}=0$. An analytic function $\vec{u}$ was chosen that satisfies this condition:

$$\vec{u} \equiv 2xy\hat{i} - \frac{1}{2}y^2\hat{j} - yz\hat{k}$$

where $\hat{i}, \hat{j}, \hat{k}$ are the unit vectors in the x, y, and z direction, respectively. A Finite Volume discretization is employed in order to compute the same gradient ($\vec{\nabla}\cdot\vec{u}$). This yields non-zero values at the nodes of the grids which are the computed error.

Figure 9 shows this error at the interface points of the hybrid grid around the fullspan plate before and after repositioning. A 12.56% reduction in the average error over all the interface points was realized. Similar results were found for the rest of the grid cases.

Specifically, Table 3 lists both the average and the maximum percentage reduction of the *computed error* for all the cases. Appreciable reduction of the average error is observed in all cases, except from the barrier one which exhibits about a 5% deterioration. In the globally refined plate case, the average error reduction was two times as much compared to its non-refined counterpart. Regarding the maximum value of the *computed error*, noticeable improvement was realized as the last column of Table 3 illustrates, with the exception of the barrier and aircraft cases where the maximum error remained constant.

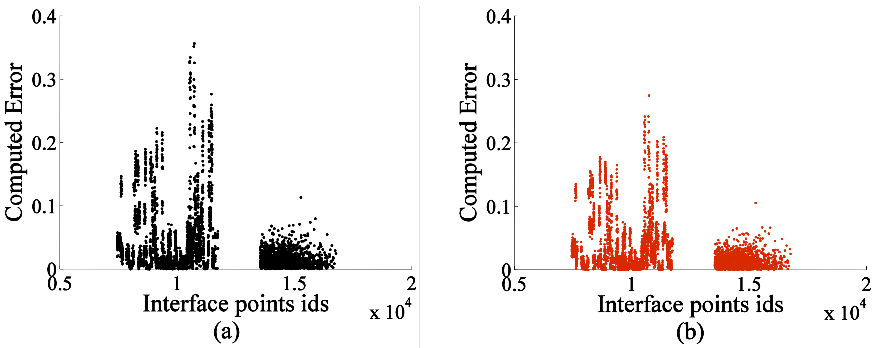

Fig. 9. Comparison of *computed error* between: (a) the initial grid, and (b) the grid following movement of the interfaces' central point. Case of a hybrid mesh around a 3-D fullspan plate.

Table 3. Effect on the *computed error* of the movement of the central interface point.

Grid interfaces	*Average* error reduction at the interfaces (%)	Reduction of the *maximum* error in interface region after applying central point movement (%)
Bump Fig.8(a)	7.17	5.00
Bump Fig.8(b)	3.35	8.33
Barrier	-4.93	0.00
Plate	19.31	8.33
Plate (refined)	38.72	30.00
Plate (fullspan)	12.56	30.00
Aircraft	2.00	0.00

5. Conclusions

The present work dealt with four distinct types of grid interfaces encountered in general hybrid meshes with variable number of elements per stack of prisms or hexahedra.

A special quality index was defined that is based on the truncation error in the calculation of solution gradients. The part that consists of grid metrics was used making this an *a priori* quality evaluation.

The quality index (Q_x, Q_y, Q_z) of the four interface types was calculated for each of the space directions. The effect of grid stretching and skewness was examined for those interfaces. The degree of sensitivity of each interface type to those distortions varies (Fig. 4 and Fig. 5).

Improvement of the quality was achieved via repositioning of the central point in each interface type. Movement towards the center of its dual volume improved the quality up to a degree of movement (Fig. 7).

Several grids, included an aircraft mesh, were employed to measure the improvement in quality at their interfaces. In most cases, both the average quality and the maximum one over all interface grid points was improved (Table 2). The same was observed with a *computed error* based on an analytic field function (Fig. 9 and Table 3).

Future work involves the improvement of the grid interface movement algorithm to be included in a constrained optimization process. Further, additional interface types that are less frequent will be studied.

References

[1] J. Thompson, Numerical Grid Generation, North-Holland, New York, 1982.
[2] T. Baker, Mesh generation for the computation of flowfields over complex aerodynamic shapes, Computers & Mathematics with Applications 24 (1992) 103–127.
[3] Y. Kallinderis, Hybrid grids and their applications, in: Handbook of Grid Generation, CRC Press, Boca Raton, FL, 1999, Chapter 35.
[4] L. Tysell, Hybrid grid generation for complex 3D geometries, in: Proceedings of the 7th International Conference on Numerical Grid Generation in Computational Field Simulations, International Society of Grid Generation (ISGG), Whistler, British Columbia, Canada, 2000, pp. 337–346 .
[5] N. Kroll, J.K. Fassbender (Eds.), MEGAFLOW—Numerical Flow Simulation for Aircraft Design, Notes on Numerical Fluid Mechanics and Multidisciplinary Design, vol. 89, Springer-Verlag, Berlin Heidelberg, 2005
[6] Y. Ito, K. Nakahashi, Improvements in the reliability and quality of unstructured hybrid mesh generation, International Journal on Numerical Method in Fluids 45 (1) (2004) 79–108.
[7] Y. Kallinderis, S. Fotia, A priori mesh quality metrics for three-dimensional hybrid grids, in Review, Journal of Computational Physics, May 2014.
[8] Y. Kallinderis, C. Kontzialis, A priori mesh quality estimation via direct relation between truncation error and mesh distortion, Journal of Computational Physics 228 (2009) 881–902.

[9] Y. Kallinderis, Numerical treatment of grid interfaces for viscous flows, Journal of Computational Physics, 98 (1992) 129–144.
[10] L. Ferm, P. Lötstedt, Accurate and stable grid interfaces for finite volume methods, Technical Report 2002-012, Department of Information Technology, Uppsala University, Uppsala, Sweden, 2002.
[11] J. Liu and W. Shyy, Assessment of grid interface treatments for multi-block incompressible viscous flow computation, Computers & Fluids, 25 (1996) 719-740.
[12] O. C. Zienkiewicz and J. Z. Zhu, The superconvergent patch recovery and a posteriori error estimates, Part 1, Part 2, International Journal for Numerical Methods in Engineering, 33 (1992) 1331-1382.
[13] D. McRae, r-Refinement grid adaptation algorithms and issues, Computer Methods in Applied Mechanics and Engineering 189 (2000) 1161–1182.
[14] Y. Kallinderis, Grid adaptation by redistribution and local embedding, in: Computational Fluid Dynamics Lecture Series 1996-06, von Karman Institute for Fluid Dynamics, Rhode Saint Genèse, Belgium, 1996.
[15] M. Thompson, An adaptive multigrid technique for the incompressible Navier–Stokes equations, Journal of Computational Physics 82 (1992) 94–121.
[16] M. Ainsworth, J.T. Oden, A posteriori error estimation in finite element analysis, Wiley-Interscience, New York, 2000.
[17] M.J. Berger, P. Collela, An adaptive multigrid method for the euler equations, Lecture Notes in Physics 218 (1985) 92–97.
[18] L.A. Freitag, P.M. Knupp, Tetrahedral element shape optimization via the Jacobian determinant and condition number, in: Proc.8th International Meshing Roundtable, Lake Tahoe, CA, 1999, Sandia Report SAND 99-2288, Sandia National Laboratories, Albuquerque, NM, 1999, pp. 247–258.
[19] P.M. Knupp, Algebraic mesh quality metrics for unstructured initial meshes, Finite Elements in Analysis and Design 39 (2003) 217–241.
[20] J.M. Escobar, R. Montenegro, G. Montero, E. Rodriguez, J. Gonzalez-Yuste, Smoothing and local refinement techniques for improving tetrahedral mesh quality, Computers and Structures 83 (2005) 2423–2430.
[21] D. Vartziotis, J. Wipper, M. Papadrakakis, Improving mesh quality and finite element solution accuracy by GETMe smoothing in solving the Poisson equation. Finite Elem. Anal. Des., 66: 36–52, 2013.
[22] T. Ikeda, P. Durbin, Mesh stretch effects on convection in flow simulations, Journal of Computational Physics 199 (2004) 110–125.
[23] E. Turkel, Accuracy of schemes with nonuniform meshes for compressible fluid flows, Applied Numerical Mathematics 2 (1986) 529–550.
[24] K.K. Okamoto, G.H. Klopfer, J.J. Chattot, Assessing grid quality of structured meshes by truncation error analysis, Fifteenth International Conference on Numerical Methods in Fluid Dynamics, vol. 490, Springer, Berlin, Heidelberg, 1997
[25] W. Lowrie, V.S. Lukin, U. Shumlak, A priori mesh quality metric error analysis applied to a high-order finite element method, Journal of Computational Physics 230 (2011) 5564–5586.
[26] CENTAUR Software - Computational Grids for Advanced Modelling. www.centaursoft.com.